Bulgarian Chemical Communications, Volume 51, Special Issue B (pp. 030 – 034) 2019 DOI: 10.34049/bcc.51.B.004

Modelling the kinetics of supercritical CO_2 extraction of biomass

R.M. Filipe[1,2,*], J.A.P. Coelho[1,3], M.P. Robalo[1,3], G.St. Cholakov[4], R.P. Stateva[5]

[1] *Instituto Superior de Engenharia de Lisboa, Instituto Politécnico de Lisboa, 1959-007 Lisbon, Portugal*
[2] *Centro de Recursos Naturais e Ambiente (CERENA), Instituto Superior Técnico, Universidade de Lisboa, 1049-001, Lisbon, Portugal*
[3] *Centro de Química Estrutural, Instituto Superior Técnico, Universidade de Lisboa, 1049-001 Lisbon, Portugal*
[4] *University of Chemical Technology and Metallurgy, 1756 Sofia, Bulgaria*
[5] *Institute of Chemical Engineering, Bulgarian Academy of Sciences, 1113 Sofia, Bulgaria*

Received: July 11, 2019; revised: August 1, 2019

This work addresses the modelling and simulation of the kinetics of CO_2 supercritical extraction of oils from biomass. Experimental and simulation results from different matrices and models are presented.

gPROMS Model Builder is used to find solutions to three different models applied to study the extraction of three different volatile oils from aromatic plants (coriander, fennel and savoury), and from a bioresidue, industrial grape seeds. The supercritical extraction experiments performed at different temperature, pressure and flow rate conditions provide the data to the modelling studies and for model parameter estimation. The qualitative and quantitative agreement between the experimental and simulated extraction profiles in terms of yields was good for the cases investigated.

Key words: supercritical CO_2 extraction, extraction kinetics, mathematical modelling, simulation, biomass valorisation.

INTRODUCTION

Nowadays, increasing attention is being drawn to the effective use of waste biomass and vegetal material as renewable sources of valuable compounds with applications in several industries, as food, cosmetics, pharmaceutical, biodiesel production, etc. While the extraction of oils from aromatic plants is well established [1–4], the use of by-products or biowastes is still underexplored. Seed biomass from *Vitis vinifera* L. is an example of underutilized biowaste. With an oil content of (8 - 15) % (w/w), rich in long chain polyunsaturated fatty acids (PUFAs) and antioxidants [5,6], and representing about (20 - 25) % of the biomass generated by the wine industry, it is still considered a disposable material and rarely valorised.

Extraction with supercritical CO_2 (SCE) has the great advantage of preventing or, at least, minimizing the degradation of bioactive compounds present in the matrix to be extracted due to the comparatively low temperatures used and oxygen free atmospheres. Furthermore, it allows obtaining solvent-free products and, unsurprisingly, is currently establishing itself as the viable, sustainable and eco-compatible alternative to the use of organic solvents. Yet, kinetic data are not abundant, and, for some systems they are scarce and superficial.

Dynamic models are a useful tool for the design, optimization and scale-up of supercritical fluid extraction processes from laboratory to pilot and industrial scales.

In particular, mass balance based models which include mass transfer coefficients in fluid and/or solid phases have a strong physical significance. They take into account the characteristics of the plant matrix, namely the particle size, the bed porosity and also the equilibrium relationships and mass transfer mechanisms.

Although several models have been proposed in the literature, their solution is not always trivial and, additionally, the estimation of some parameters using experimental data is required. Within this context, the opportunity to use new tools to model, simulate and perform parameter estimation seems promising.

In view of the above, the aim of our work is to model the kinetics of the SCE of oils from aromatic plants, namely, coriander, fennel, and savoury, and from a biowaste - industrial grape seeds, obtained directly from a Portuguese industry, by applying an efficient solution method to different models.

METHODOLOGY

The extraction conditions and the experimental results were previously reported for the aromatic plants [7] and the grape seeds [8]. For the aromatic plants, the simulation results presented by Grosso et al. [7] are used as comparison in order to evaluate the efficiency of the solution method used in this work.

The models were implemented in gPROMS ModelBuilder [9], an equation-oriented modelling

* To whom all correspondence should be sent:
E-mail: rfilipe@isel.ipl.pt

and optimisation platform for steady-state and dynamic systems, and the experimental data was used to obtain the model parameters using gPROMS parameter estimation.

The desorption model by Tan and Liou [10] and the model proposed by Sovová [11], both without axial dispersion are used for the aromatic plants. These models consider the variation of the concentration of the supercritical fluid as it flows along the extractor and, thus, include partial differential equations.

The model by Tan and Liou [10], from now on referred to as model 1, is described by:

$$\frac{\partial C}{\partial t}+\frac{u}{\varepsilon}\frac{\partial C}{\partial h}+\frac{1-\varepsilon}{\varepsilon}\frac{\rho_s}{\rho_f}\frac{\partial q}{\partial t}=0 \quad (1)$$

$$\frac{\partial q}{\partial t}=-k_d q \quad (2)$$

With the initial and boundary conditions defined by:

$$q(h,0)=q_0 \quad (3)$$

$$C(h,0)=C_0 \quad (4)$$

$$C(0,t)=0 \quad (5)$$

Where C is the concentration in the fluid phase, t is time in minutes, u is the superficial velocity of supercritical fluid ($m \cdot s^{-1}$), ε is the bed void fraction, ρ_s and ρ_f are the density of the solid and fluid phase ($kg \cdot m^{-3}$), q is the solute concentration in the solid phase ($kg \cdot kg^{-1}$) and k_d is the desorption coefficient (s^{-1}).

The model by Sovová [11], from now on referred to as model 2, is described by:

$$\frac{\partial C}{\partial t}+\frac{u}{\varepsilon}\frac{\partial C}{\partial h}+\frac{1-\varepsilon}{\varepsilon}\frac{\rho_s}{\rho_f}\frac{\partial q}{\partial t}=0 \quad (6)$$

$$\frac{\partial q}{\partial t}=-\frac{k_f a \rho_f}{\rho_s}(C_0-C), \qquad q \geq q_k \quad (7)$$

$$\frac{\partial q}{\partial t}=-k_s a q, \qquad q < q_k \quad (8)$$

With the following initial and boundary conditions:

$$q(h,0)=q_0 \quad (9)$$

$$C(h,0)=C_0 \quad (10)$$

$$C(0,t)=0 \quad (11)$$

Where q_k is the initial content of the difficult accessible solute in the solid ($kg \cdot kg^{-1}$), a is the surface of a unit volume of particles (m^{-1}), and k_s and k_f are the internal and external mass transfer coefficients.

The third model used in this work, model 3, developed by Sovová and Stateva [12], is described by the following set of equations:

$$\frac{dw}{dt}+\frac{w}{t_r}=\frac{k_f a_0}{\varepsilon}\left(w^+-w\right) \quad (12)$$

$$\frac{dw_s}{dt}=-q' t_r \frac{k_f a_0}{\varepsilon}\left(w^+-w\right) \quad (13)$$

$$w^+=K w_s+\frac{w_s^b}{w_t^b+w_s^b}(w_{sat}-K w_s) \quad (14)$$

With the initial conditions:

$$w(0)=w_0 \quad (15)$$

$$w_s(0)=w_{s,0} \quad (16)$$

The yield, e ($kg \cdot kg^{-1}$ solid), is defined by:

$$e=q'\int_0^t e dt \quad (17)$$

$$e(0)=0 \quad (18)$$

Where w is the oil concentration in the fluid phase inside the extractor ($kg \cdot kg^{-1}$ CO_2), w_s is the oil concentration in the solid phase ($kg \cdot kg^{-1}$ solid), t and t_r are the extraction and residence time (min), respectively, q' is the specific flow rate (kg $CO_2 \cdot min^{-1} \cdot kg^{-1}$ solid), w^+ is the oil concentration at solid-fluid interface ($kg \cdot kg^{-1}$ CO_2), ε is the void fraction in the bed, $k_f a_0$ (min^{-1}) is the volumetric fluid phase mass transfer resistance, K is the partition coefficient, w_t ($kg \cdot kg^{-1}$ CO_2) is the monolayer adsorption maximum content, w_{sat} ($kg \cdot kg^{-1}$ CO_2) is the solubility of the free oil compound, and b is a coefficient that should be higher than one.

This model considers homogeneous concentration in the extractor at both solid and fluid phases and assumes that the extracts are located on the surface of the solid particles. Thus, the extracts overcome only the external mass transfer resistance, which is usually much smaller than the internal resistance. This assumption allows neglecting internal diffusion, which is compatible with finely ground substrates where the diffusion path in the particles is short and the extract is easily accessible, resulting in negligible internal mass transfer resistance.

The grape seeds are very complex mixtures of mainly triacylglycerols (TAG) with minor amounts of other compounds. Due to this complexity the grape seeds oil is usually represented by a single model TAG, and, for the purposes of modelling and comparison with the results of other authors [8] triolein was selected to exemplify the oil. Model 3 requires solubility data of the model TAG in the supercritical CO_2, which was calculated applying the predictive Soave-Redlich-Kwong (PSRK) cubic EoS [13].

gPROMS Modelbuilder parameter estimation with MAXLKHD solver was used to estimate the desorption rate constant (k_d) for model 1, the internal and external mass transfer coefficients (k_s and k_f) for model 2, and the partition coefficient (K) for model 3. gPROMS uses a maximum likelihood parameter estimation problem and attempts to determine values for the uncertain physical and

variance model parameters that maximize the probability that the mathematical model will adequately predict the values obtained from the experiments.

To apply model 3 to grape seeds, the value of k_f was calculated following [8], where the relation proposed by [14] was used. The values obtained were 6.77E-4 and 6.95E-4 for T = (313 and 333) K, respectively. Parameter b was set to 7 [12] and w_t was set to 60% of the initial concentration of the oil in the grape seeds.

In order to compare the fitting accuracy obtained with other works, two standard deviation measures were calculated after parameter estimation: the absolute average relative deviation, AARD, defined by Eq. (19), and the root mean square deviation, RMSE, defined by Eq. (20), where N is the total number of experimental points, and e_i^{exp} and e_i^{est} - the i-th experimental and estimated point, respectively.

$$\text{AARD} = \frac{100}{\text{N}} \sum_{j=1}^{N} \frac{\left| e_i^{exp} - e_i^{est} \right|}{e_i^{exp}} \tag{19}$$

$$\text{RMSE} = \sqrt{\frac{1}{N}\left(e_i^{exp} - e_i^{est}\right)^2} \tag{20}$$

RESULTS AND DISCUSSION

After the estimation of the parameters for each of the models used (k_d for model 1, k_s and k_f for model 2 and K for model 3), an analysis of the yield profiles was performed. The quality of the fitting obtained with parameter estimation was also evaluated and, for the aromatic plants, compared with previously reported results [7]. The yield profiles are presented as a set of data points, obtained experimentally and with parameter estimation. The lines connecting the points were included to improve readability and do not represent simulation results.

On Figure 1 the yield of extraction *versus* time is shown for coriander. The experimental data, the simulation results reported in [7] and the ones obtained in this work using the models from Sovová, and Tan and Liou are depicted. Although some limitations were encountered in parameter estimations due to the limited amount of data available, the results obtained improved the ones previously reported for the aromatic plants [7], as assessed by the absolute deviation error (Table 1).

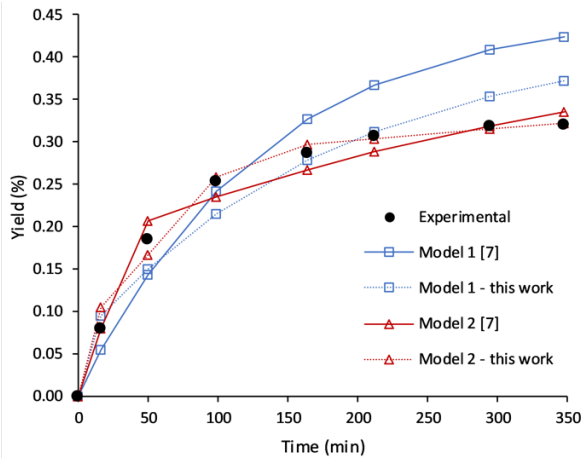

Fig. 1. Experimental and simulated extraction profiles for coriander P = 9 MPa, T = 313 K, P_{size} = 0.6 mm, F = 6 L/min.

The results for savoury using model 1 and 2 are displayed in Figure 3. Model 2 performs better, when compared to model 1, with a lower AARD (Table 1), and the results obtained in this work reduce the AARD by approximately 50 %.

For the fennel system (Figure 4), the AARD previously reported [7] is quite small for model 2, and could not be improved further. A reason for not improving might be that the AARD has reached the experimental reproducibility of the data being modelled.

Table 1. Parameter estimation results for the systems studied

System	Model	P (MPa)	T (K)	F (L·min^{-1})	P_{size} (mm)	k_d (s^{-1})	k_f (m·s^{-1})	k_s (m·s^{-1})	K	RMSE (%)	AARD (%)	AARD (%) [7]
Coriander	1	9	313	6	0.6	5.1E-05				2.9E-02	10.7	19.0
Coriander	1	9	313	8	0.6	1.7E-04				2.6E-02	7.1	14.9
Coriander	2	9	313	6	0.6		1.8E-07	2.6E-09		1.2E-02	6.3	5.3
Coriander	2	9	313	8	0.6		2.3E-06	1.3E-08		1.5E-02	3.3	3.2
Savoury	1	9	313	6	0.6	1.7E-04				2.9E-01	9.3	18.7
Savoury	2	9	313	6	0.6		8.2E-03	4.6E-08		6.0E-02	3.4	6.5
Fennel	1	9	313	6	0.6	2.4E-04				1.5E+00	7.3	10.0
Fennel	2	9	313	6	0.6		9.8E-06	9.3E-08		1.0E-01	3.6	2.1
Grape seeds	1	40	313	1	0.6	1.4E-04				2.4E+00	26.7	
Grape seeds	1	40	333	1	0.6	1.6E-04				2.6E+00	28.7	
Grape seeds	3	40	313	1	0.6				0.22	5.0E-01	4.5	
Grape seeds	3	40	333	1	0.6				0.43	7.0E-01	8.6	

Figure 2 depicts the extraction profiles with two different flows of supercritical CO_2, and an increase in the speed of extraction is observed when the flow increases. Once again, an improvement in the fitting was achieved with the methodology used in this work.

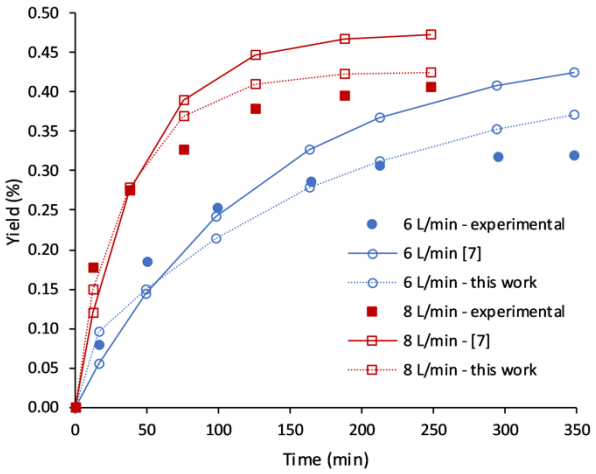

Fig. 2. Extraction profiles for coriander using model 1. P = 9 MPa, T = 313 K, P_{size} = 0.6 mm, F = (6 and 8) L/min.

The results obtained demonstrate the good performance of gPROMS ModelBuilder, which was able to improve the AARD for almost all cases investigated.

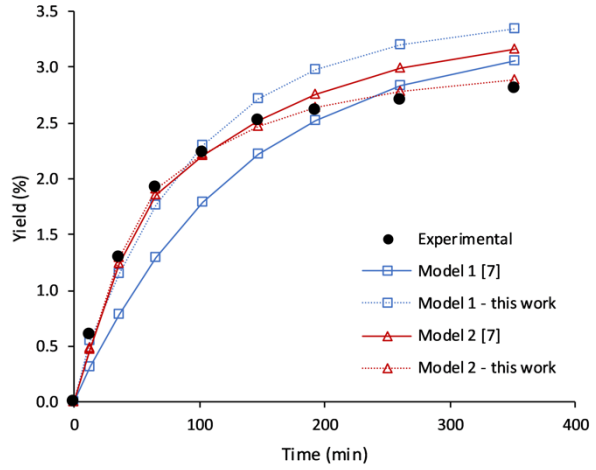

Fig. 3. Experimental and simulated extraction profiles for savoury. P = 9 MPa, T = 313 K, P_{size} = 0.6 mm F = 6 L/min.

Figure 5 shows the profiles for the grape seeds extraction, where the temperature is different for each case. The increase in temperature results in a faster extraction.

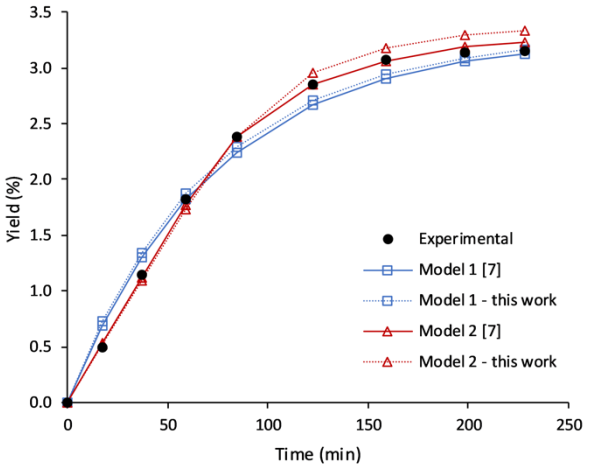

Fig. 4. Experimental and simulated extraction profiles for fennel P = 9 MPa, T = 313 K, P_{size} = 0.6 mm F = 6 L/min.

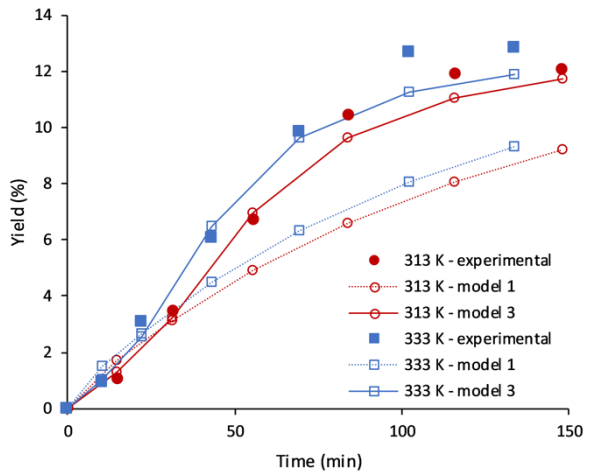

Fig. 5. Experimental and simulated extraction profiles for grape seeds using models 1 and 3. P = 40 MPa, P_{size} = 0.6 mm F = 1 L/min, T = (313 and 333) K.

Model 3 is much more effective fitting the experimental data than model 1, for both cases. Indeed, the high AARD obtained with model 1, indicates that this model is not adequate for grape seeds extraction simulation. Model 3 incorporates in a rigorous way the interplay between phase equilibria (solubility) and kinetics, and the results obtained demonstrate that albeit the simplifications introduced in representing the grape seeds oils by just a single model TAG, there is a good qualitative and quantitative agreement between the experimental and calculated extraction yields at the SCEs operating conditions examined. It should be emphasized that although the internal diffusion is neglected, the model can still deliver adequate results, providing that the particle size is small, as is the case for the matrix used in this work.

CONCLUSIONS

This work presents the results from modelling the kinetics of SCE of biomass from three aromatic plants and industrial grape seeds, obtained directly from a Portuguese industry without preliminary treatment. The influence of the operating conditions on the extraction yield was analysed for some of the systems and reported.

To simulate the extraction kinetics, three different models were used. The model equations were integrated using gPROMS ModelBuilder and the results were compared to previously reported data. Models 1 and 2 are show to be adequate for the aromatic plants investigated, with AARD values in the range (3.3 – 10.7) %. However, they could not simulate adequately the grape seeds kinetics, as demonstrated by the large AARD obtained. For model 3, the qualitative and quantitative agreement between the experimental and simulated extraction profiles in terms of yields for the grape seeds was quite adequate taking into consideration the complex nature of the systems examined. The good fitting results also indicate that the model can be successfully used in finely ground matrices where the internal diffusion contribution to the extraction phenomena is very small and, thus, negligible.

Acknowledgements: *The authors acknowledge the funding received from the European Union's Horizon 2020 research and innovation programme under the Marie Sklodowska-Curie grant agreement No 778168. J. A. P. Coelho and R. M. Filipe are thankful for the financial support from Fundação para a Ciência e a Tecnologia, Portugal, under projects UID/QUI/00100/2019; UID/ECI/04028/2019.*

REFERENCES

1. M. Poletto, E. Reverchon, *Ind. Eng. Chem. Res.*, **35**, 3680 (1996).
2. E. Reverchon, I. De Marco, *J. Supercrit. Fluids*, **38**, 146 (2006).
3. K. Mechergui, W. Jaouadi, J. P. Coelho, M. L. Khouja, *Ind. Crops Prod.*, **90**, 32 (2016).
4. J. Coelho, J. Veiga, A. Karmali, M. Nicolai, C. Pinto Reis, B. Nobre, A. Palavra, *Separations*, **5**, 21 (2018).
5. S. Bail, G. Stuebiger, S. Krist, H. Unterweger, G. Buchbauer, *Food Chem.*, **108**, 1122 (2008).
6. L. Fernandes, S. Casal, R. Cruz, J. A. Pereira, E. Ramalhosa, *Food Res. Int.*, **50**, 161 (2013).
7. C. Grosso, J. P. Coelho, F. L. P. Pessoa, J. M. N. A. Fareleira, J. G. Barroso, J. S. Urieta, A. F. Palavra, H. Sovová, *Chem. Eng. Sci.*, **65**, 3579 (2010).
8. J. P. Coelho, R. M. Filipe, M. P. Robalo, R. P. Stateva, *J. Supercrit. Fluids*, **141**, 68 (2018).
9. Process Systems Enterprise, gPROMS, www.psenterprise.com/gproms, 1997-2019.
10. C. S. Tan, D. C. Liou, *AIChE J.*, **35**, 1029 (1989).
11. H. Sovova, *Chem. Eng. Sci.*, **49**, 409 (1994).
12. H. Sovova, R. P. Stateva, *Ind. Eng. Chem. Res.*, **54**, 4861 (2015).
13. T. Holderbaum, J. Gmehling, *Fluid Phase Equilib.*, **70**, 251 (1991).
14. C. R. Wilke, P. Chang, *AIChE J.*, **1**, 264 (1955).